

## Synthesis and Characterization of Fe<sub>3</sub>O<sub>4</sub>@APTES@MOF-199 Magnetic Nanocatalyst and Its Application in the Synthesis of Quinoxaline Derivatives

Sami Sajjadifar\*, Issa Amini, Mina Karimian

Department of Chemistry, Payame Noor University, PO BOX 19395-4697 Tehran, Iran

Received 5 August 2020; received in revised form 18 December 2020; accepted 10 January 2021

### ABSTRACT

In this research, design and synthesis of Fe<sub>3</sub>O<sub>4</sub>@APTES@MOF-199 magnetic nanocatalyst nanoparticles as a novel, recyclable and heterogeneous catalyst was developed. The magnetic nanocatalyst was analyzed using various spectroscopic methods such as Fourier transform infrared spectroscopy (FTIR), scanning electron microscopy (SEM), powder X-ray diffraction (XRD), energy dispersive X-ray (EDX), thermogravimetric analysis (TGA), vibrating sample magnetometer (VSM). The particle size of the nanocatalyst is about 15-96 nm. In addition, magnetic nanocatalysts have been successfully applied to the synthesis of quinoxaline derivatives with a range of derivatives. The crude compounds were isolated in 84-97% yields. The recyclability of the catalyst was evaluated up to 5 times, with no loss in catalysis activity.

**Keywords:** Metal-organic framework, Fe<sub>3</sub>O<sub>4</sub>@APTES@MOF-199, Quinoxaline, Nanocatalyst.

### 1. Introduction

In the field of catalytic knowledge, achieving high activity and selectivity for performing a catalytic reaction is a challenging issue [1]. Also, recovering and reusing a typical catalytic system for presenting a sustainable process are vital factors. Although homogeneous catalysts, from the point of view of activity and selectivity are very desirable, troublesome separation from the reaction media limited their potential applications both in industrial and laboratory processes. It has been proven that the combination of nanochemistry knowledge and heterogenization of small catalytic species on special supports can resolve these problems. One of the best options for this process is employing magnetic nanoparticles as support for the construction of heterogeneous catalytic systems. Nano magnetic based heterogeneous catalytic systems have a high surface-to-volume ratio which guarantees the high activity of the catalytic system. These catalysts can also be easily separated from the reaction media by using a simple external magnet. These features make nano magnetic based heterogeneous catalytic systems a great option for both industrial and academic chemists [2-6].

In the last decade, the use of some crystalline materials such as metal-organic framework (MOFs) as heterogeneous catalysts has become conventional due to the high surface-to-volume ratio, regular cavity diameter, acid sites, base sites, stability, diffusion, high metal content, recyclability and high selectivity [7-10]. These compounds have attracted much attention, due to new coordinated structures, different topologies and potential applications in the storage of gases (such as hydrogen, methane, acetylene, carbon dioxide and oxygen), component separation, catalytic processes, drug delivery, molecular identification, luminescence, magnetism and conductivity [11]. Metal-organic frameworks have a regular structure, consisting of metal and organic ligands, and the pore structure is such that it can be designed by chemical engineering for a specific application [12]. Recently, metal-organic frameworks are used as solid and heterogeneous catalysts or as substrates for the conversion of different functional groups [13]. Some of the reactions carried out by metal-organic frameworks are as follows, Friedel-Crafts alkylation and acylation [14], oxidation [15], epoxidation of alkenes [16], Suzuki cross coupling reaction [17], Sonogashira reaction [18], esters exchange reaction [19], Novoagle condensation reaction [20], and ring opening of epoxides [21]. Compared to

\*Corresponding author:

E-mail address: [ss\\_sajjadifar@yahoo.com](mailto:ss_sajjadifar@yahoo.com) (S. Sajjadifar)

conventional microporous and mesoporous minerals used, these metal-organic frameworks have greater potential in flexibility and reaction design by controlling the structure and functionalizing the holes [22]. The magnetic MOFs have been used as sustainable environment adsorbents [23], efficient removal of organic dyes from water [24], selective removal of chromium (VI), cadmium (II) and lead (II) [25] etc. The magnetic MOFs catalyst for the organic reaction has been very limited in the literature. Building of magnetic MOFs is a good example through growth of MOF with magnetic particles, which can be used in the area of heterogeneous catalysts [26].

Among the heterocyclic compounds, quinoxaline and their derivatives are important compounds due to biological and pharmacological properties which perform antifungal [27], insecticide [28], antibacterial [29], anticancer, antimalarial, anti-HIV [30] and antibiotics [31] activities. Quinoxaline derivatives are also used in industry, fluorescent dyes, materials with electroluminescence properties, and the synthesis of organic semiconductors [32]. The methods reported in the literature for the synthesis of quinoxaline utilize various catalytic systems such as ultrasonic [33],  $\text{CuSO}_4 \cdot 5\text{H}_2\text{O}$  (II) [34], heteropoly acids [35], Si/MCM-41 [36], phosphosulfonic acid [37], boron sulfonic acid [38], citric acid [39], bismuth (III) triflate [40], ammonium chloride [41], Zn(L-proline) [42] etc.

Continuing our efforts to synthesize novel nanomagnetic catalysts, we prepared  $\text{Fe}_3\text{O}_4@ \text{APTES}@ \text{MOF}-199$  magnetic nanocatalyst and fully characterized it. We tended to evaluate the catalytic activity of  $\text{Fe}_3\text{O}_4@ \text{APTES}@ \text{MOF}-199$  magnetic nanocatalyst for the one-pot reaction of quinoxaline derivatives *via* condensation reactions between 1,2-dicarbonyl and *o*-phenylenediamines in ethanol at room temperature. This methodology presents a lot of benefits compared with the previous methods, such as good to excellent yields, low cost, short reaction time and ready availability.

## 2. Experimental

### 2.1. General

All solvents and reagents used in this work were obtained from Merck Company and were used without further purification. Analytical thin-layer chromatography was performed using Merck silica gel GF<sub>254</sub> plates. The <sup>1</sup>H NMR ( $\text{CDCl}_3$ , 400 MHz) and <sup>13</sup>C NMR ( $\text{CDCl}_3$ , 100 MHz) spectra were recorded with BRUKER AVANCE instruments. The XRD spectra were recorded on an X'Pert Pro instrument from Panalytical Company. The SEM were recorded by ZEISS Company, SIGMA VP model. The VSM was

recorded by the Meghnatis Daghigh Kavir Company, LBKFB model.

### 2.2. Preparation of $\text{Fe}_3\text{O}_4@ \text{APTES}@ \text{MOF}-199$ magnetic nanocatalyst

5.84 g (0.0216 mol) of  $\text{FeCl}_3 \cdot 6\text{H}_2\text{O}$  and 2.17 g (0.0108 mol) of  $\text{FeCl}_2 \cdot 4\text{H}_2\text{O}$  were dissolved in 100 mL deionized water at 80 °C under nitrogen gas atmosphere with vigorous stirring for 30 minutes. Then, 10 mL of 25% aqueous ammonia solution was added dropwise at 80 °C under nitrogen gas atmosphere that resulted in the formation of uniform black  $\text{Fe}_3\text{O}_4$  magnetic nanoparticles. The resulting black mixture was stirred under nitrogen gas atmosphere for 30 min. The reaction mixture was then allowed to cool to room temperature and the resulting black precipitate was separated using an external magnet and washed several times with distilled water. Magnetic iron nanoparticles were isolated and dried at room temperature for 24 h.  $\text{Fe}_3\text{O}_4$  (3.0 g) was dispersed in 40 mL ethanol and was sonicated for 30 min. Then, 5 mL 3-aminopropyltriethoxysilane (APTES) (21.36 mmol) was added to the suspended solid nanoparticles under stirring, and the reaction mixture was refluxed under nitrogen for 8 h. Amino propyl modified magnetic nanoparticles ( $\text{Fe}_3\text{O}_4@ \text{APTES}$ ) was filtered, washed twice with EtOH and dried in vacuum at 50 °C [43]. In the third step,  $\text{Cu}(\text{NO}_3)_2 \cdot \text{H}_2\text{O}$  0.221 g (0.9 mmol) was dissolved in 3 ml of distilled water. Trimesic acid (benzene-1,3,5-tricarboxylic acid, 0.105 g (0.5 mmol) add to 3.0 mL of ethanol, and mix thoroughly for 20 minutes by a magnetic stirrer. Then, 0.01 g of dispersed  $\text{Fe}_3\text{O}_4@ \text{APTES}$  was added to the reaction mixture. The mixture was sonicated for 20 minutes. It was then incubated reaction in an autoclave reactor at 100 °C for 12 h. Finally, the obtained  $\text{Fe}_3\text{O}_4@ \text{APTES}@ \text{MOF}-199$  was washed several times with water and ethanol. The resulting catalyst was completely dried overnight at 60 °C.

### 2.3. General procedure for the synthesis of quinoxaline derivatives

In a 20 mL round bottom balloon, a mixture of *o*-phenylenediamine (1 mmol) and 1,2-dicarbonyl (1 mmol) was stirred in the presence of magnetic catalysts (10 mg) in 5 mL of ethanol as solvent at room temperature was stirred. The reaction progress was monitored by thin layer chromatography (TLC). The reaction continued until the completion of reaction. Upon completion of the reaction, the catalyst was separated by applying an external magnetic field, and the remainder of the mixer reaction was obtained by recrystallization with hot ethanol and then the product was recovered with high efficiency.

#### 2.4. Selected characterization data

2,3-diphenylquinoxaline: White Crystal, m.p. 129-131 °C.  $^1\text{H}$  NMR ( $\text{CDCl}_3$ , 400 MHz):  $\delta$  7.35-8.23 (14 H, m).  $^{13}\text{C}$  NMR ( $\text{CDCl}_3$ , 100 MHz):  $\delta$  153.6, 141.2, 139.2, 130.1, 130.0, 129.4, 129.0, and 128.4 ppm.

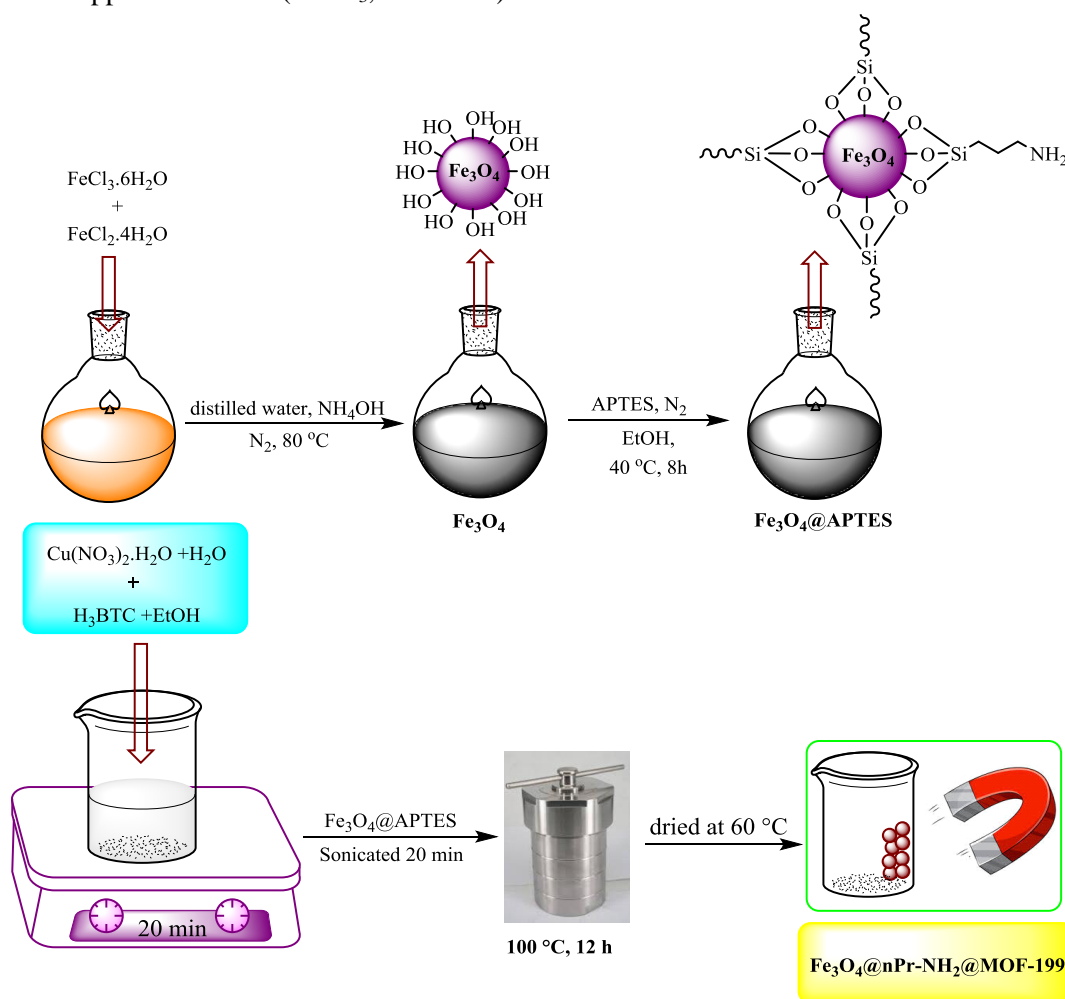
6-bromo-2,3-diphenylpyrido[2,3-b]pyrazine: Green pale crystal, m.p. 114-115 °C.  $^1\text{H}$  NMR ( $\text{CDCl}_3$ , 400 MHz):  $\delta$  7.33-7.64 ppm.  $^{13}\text{C}$  NMR ( $\text{CDCl}_3$ , 100 MHz):

$\delta$  156.6, 155.6, 155.2, 148.4, 139.5, 138.2, 138.0, 130.3, 130.0, 129.8, 129.7, 128.6, and 128.4 ppm.

### 3. Results and Discussion

#### 3.1. Preparation and characterization of catalyst

The synthetic pathway for the preparation of heterogeneous  $\text{Fe}_3\text{O}_4@\text{APTES}@ \text{MOF-199}$  magnetic nanocatalyst was shown in **Scheme 1**.



**Scheme 1.** Preparation of  $\text{Fe}_3\text{O}_4@\text{APTES}@ \text{MOF-199}$  magnetic nanocatalyst

The scanning electron microscopy (SEM) image was used to verify the morphology of the  $\text{Fe}_3\text{O}_4@\text{APTES}@ \text{MOF-199}$  magnetic nanocatalyst. **Fig. (1a)** shows SEM image for MOF-199 and **Fig. (1b)** shows SEM image for  $\text{Fe}_3\text{O}_4$  with spherical structure, which according to reported previous literature [44a]. **Figs. (c, d)** are the images after the  $\text{Fe}_3\text{O}_4$  magnetic nanoparticles are exposed on the surface of MOF-199. The particle size of the nanocatalyst is about 15-96 nm. **Fig. 2** shows the FT-IR spectra of (a)  $\text{Fe}_3\text{O}_4$ , (b)  $\text{Fe}_3\text{O}_4@\text{APTES}$ , and (c)  $\text{Fe}_3\text{O}_4@\text{APTES}@ \text{MOF-199}$ . The FT-IR spectrum of  $\text{Fe}_3\text{O}_4$  nanoparticles (**Fig. 2a**) shows the  $579\text{ cm}^{-1}$  and  $444\text{ cm}^{-1}$  peaks in that are related

to the vibration of Fe-O bonds. Also, peaks above  $3000\text{ cm}^{-1}$  are related to vibrations of OH bands present on the surface of the nanoparticles and in **Fig. 2b**  $3421\text{ cm}^{-1}$  and  $3301\text{ cm}^{-1}$  are related to the vibration of the amine groups. In **Fig. 2c**, the peaks of  $2859\text{ cm}^{-1}$  and  $2929\text{ cm}^{-1}$  are related to the vibrations of the C-H bonds. The acidic peak of the  $\text{H}_3\text{BTC}$  corresponding to the structure of the MOF-199 appeared well at  $\text{cm}^{-1}$ . Also, the peak of  $1171\text{-}1105\text{ cm}^{-1}$  is related to the vibrations of Fe-Si-O and O-Si-O bonds.

X-ray diffraction results of  $\text{Fe}_3\text{O}_4$ , MOF-199 and  $\text{Fe}_3\text{O}_4@\text{APTES}@ \text{MOF-199}$  samples are shown in **Fig. 3**. The XRD pattern of  $\text{Fe}_3\text{O}_4$  shows that the diffraction

peaks of the crystal plates (220), (311), (222), (110), (422), (511), (440), (620) and (533).  $\text{Fe}_3\text{O}_4$  has a spherical structure and is compatible with the standard card (ICDD card No 19-0629) [44b]. XRD pattern of MOF-199 is compatible with the pattern presented in previous studies [44c]. In the XRD pattern of  $\text{Fe}_3\text{O}_4$ @APTES@MOF-199, the peaks of  $\text{Fe}_3\text{O}_4$  and MOF-199 structure are found.

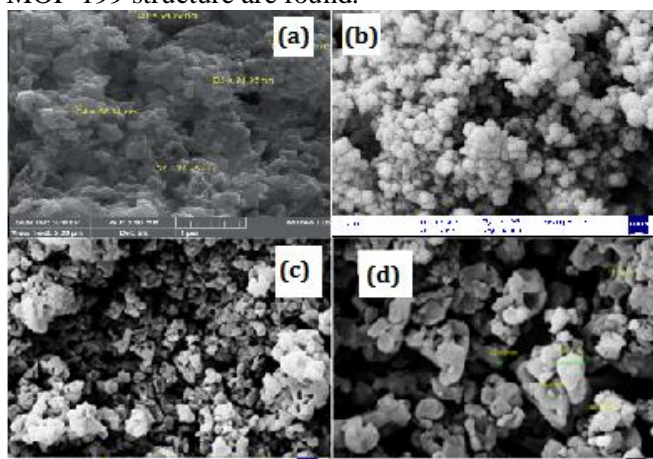


**Fig. 1.** SEM image of (a) MOF-199, (b)  $\text{Fe}_3\text{O}_4$ , (c) and (d)  $\text{Fe}_3\text{O}_4$ @APTES@MOF-199

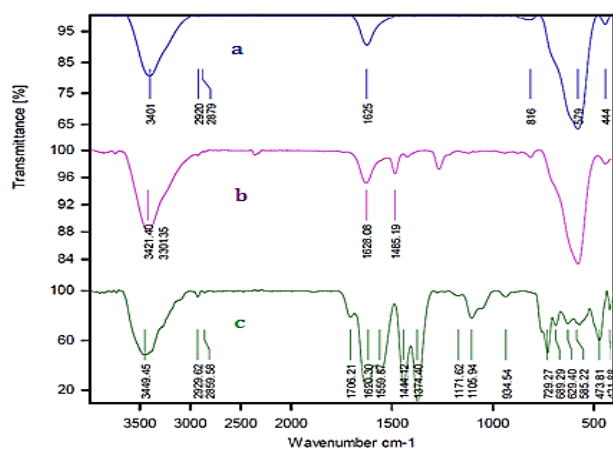


**Fig. 2.** FT-IR spectra of (a)  $\text{Fe}_3\text{O}_4$ , (b)  $\text{Fe}_3\text{O}_4$ @APTES, and (c)  $\text{Fe}_3\text{O}_4$ @APTES@MOF-199

The energy dispersive X-ray (EDX) spectrum shows clearly the presence of Fe, O, N, C, Si, and Cu elements in the nanomagnetic catalyst. The presence of copper peak in the EDX spectrum confirmed the synthesis of  $\text{Fe}_3\text{O}_4$ @APTES@MOF-199 (**Fig. 4**).

To investigate the stability and the presence of organic structure on  $\text{Fe}_3\text{O}_4$ @APTES@MOF-199, thermogravimetric analysis (TGA) was performed under  $\text{N}_2$  atmosphere in the range of 25–600 °C. A weight loss at 150 °C is suggested due to removal of trapped solvents such as water. Also, a weight loss of around 44% up to 200–300 °C is suggested to be due to removal of organic functional groups. As TGA analysis curves show that decomposition of  $\text{Fe}_3\text{O}_4$  magnetic

nanoparticles started at 320 °C. Therefore, obtained data show high thermal stability in elevated temperatures (**Fig. 5**).

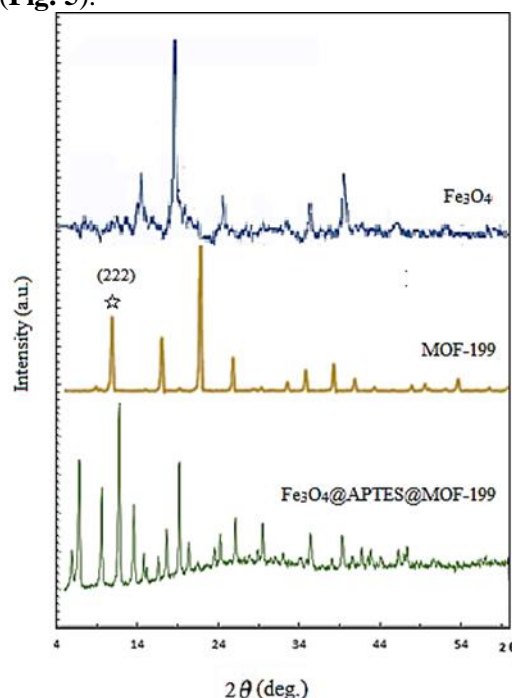


**Fig. 3.** The X-ray diffraction of  $\text{Fe}_3\text{O}_4$ @APTES@MOF-199

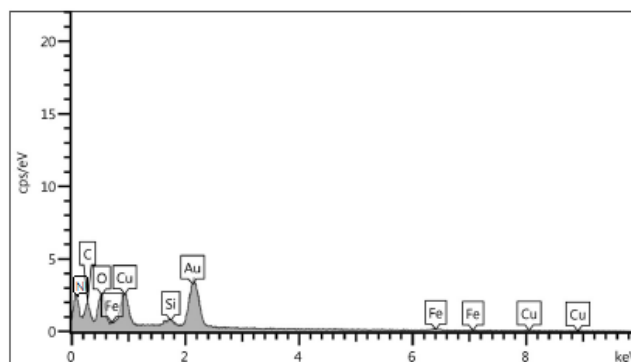


**Fig. 4.** The energy dispersive X-ray (EDX) analyzes of  $\text{Fe}_3\text{O}_4$ @APTES@MOF-199

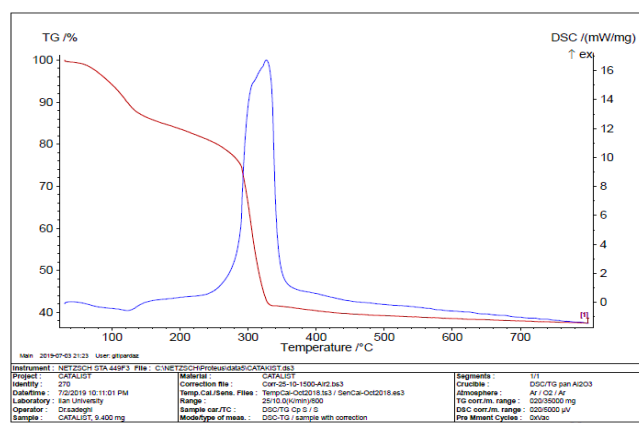


**Fig. 5.** TGA analyzes of  $\text{Fe}_3\text{O}_4$ , MOF-199 and  $\text{Fe}_3\text{O}_4$ @APTES@MOF-199

The magnetic properties of prepared catalyst and  $\text{Fe}_3\text{O}_4@APTES@MOF-199$  were investigated by applying VSM analysis (**Fig. 6**). In the VSM, the saturation magnetization of  $\text{Fe}_3\text{O}_4@APTES@MOF-199$  is about  $17.64 \text{ emu g}^{-1}$ , which is lower than  $\text{Fe}_3\text{O}_4$  nanoparticles about  $47.79 \text{ emu g}^{-1}$  [45].

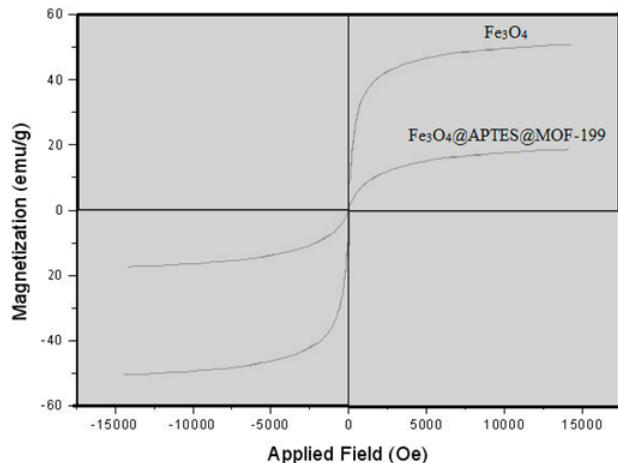


**Fig. 6.** VSM analyzes of  $\text{Fe}_3\text{O}_4$  and  $\text{Fe}_3\text{O}_4@APTES@MOF-199$

### 3.2. Catalytic studies

After characterizing the novel catalyst, we initially studied *o*-phenylenediamine and benzyl reaction as a model to find the optimized reaction conditions. For this

goal we screened the model reaction in the presence of various catalyst loading and different solvents and found that the best results were obtained in the presence of 10 mg of novel nano magnetic catalyst in EtOH as a benign green solvent (**Table 1**, Entry 1). Evidently, in the lack of the catalyst, the reaction could not progress by 12 h (**Table 1**, entry 8).

To generalize this methodology, a series of quinoxaline were subjected to  $\text{Fe}_3\text{O}_4@APTES@MOF-199$  as heterogeneous magnetic nanocatalyst in ethanol at room temperature. Many types of 1,2-dicarbonyl and *o*-phenylenediamines were used to obtain the corresponding products in very good yields (**Table 2**).

In **Scheme 2**, the plausible reaction mechanism of  $\text{Fe}_3\text{O}_4@APTES@MOF-199$  is demonstrated. Carbonyl groups in diketone are activated by catalyst. Then diketone reacts readily with *o*-phenylenediamine. The resultant amino-1,2-diol undergoes dehydration to give quinoxaline as the end product.

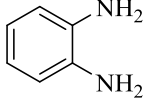
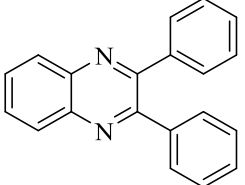
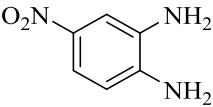
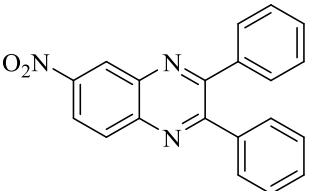
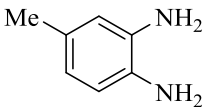
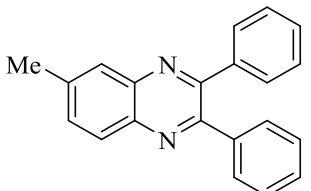
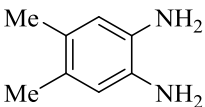
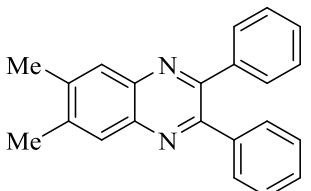
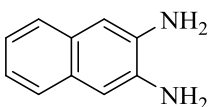
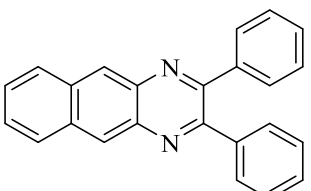
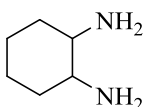
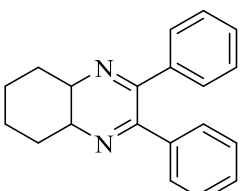
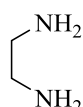
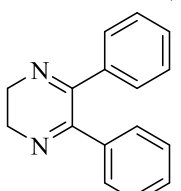
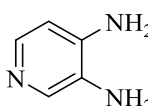
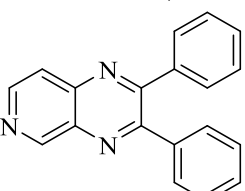
Additionally, the recovering and reusing capacity of the prepared novel acidic nanomagnetic catalyst were checked using the reaction of *o*-phenylenediamine and benzyl under optimized reaction conditions. After five consecutive runs, there is no considerable reduction in the yield observed.

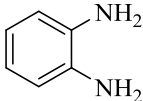
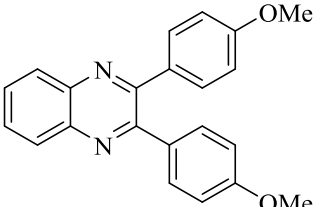
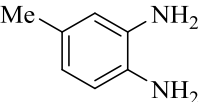
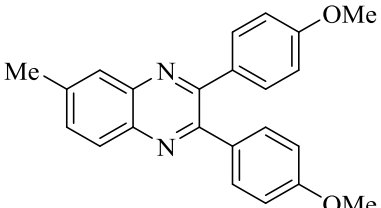
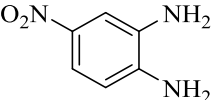
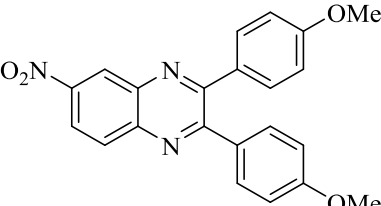
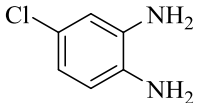
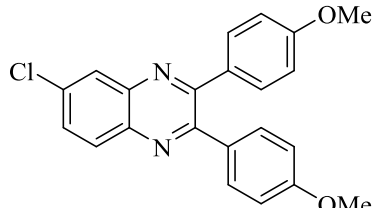
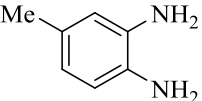
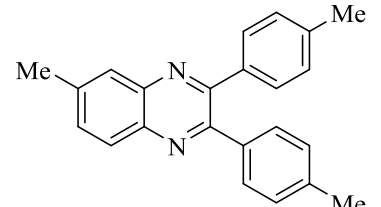
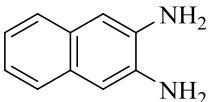
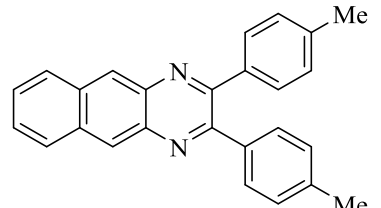
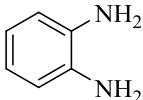
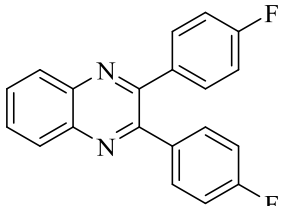
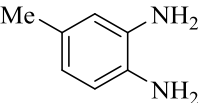
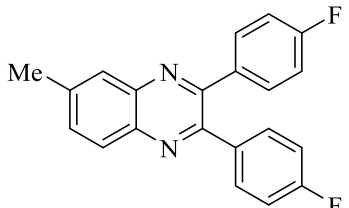
**Table 1.** Optimal conditions for the synthesis of quinoxaline in the presence of  $\text{Fe}_3\text{O}_4@APTES@MOF-199$

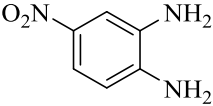
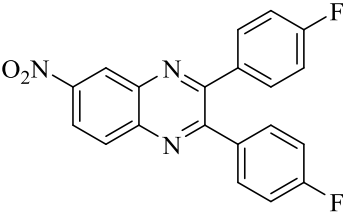
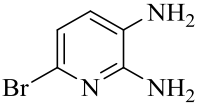
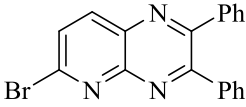
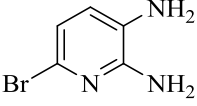
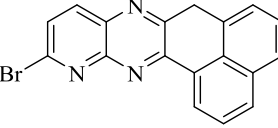
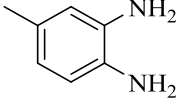
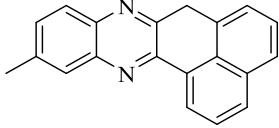
Entry	Solvent	Amounts of catalyst (mg)	Time (min)	Yield (%) <sup>a</sup>
1	EtOH	10	20	<b>94</b>
2	H <sub>2</sub> O	10	45	21
3	CH <sub>3</sub> Cl	10	30	78
4	EtOAc	10	30	71
5	MeOH,	10	30	60
6	EtOH	7	20	49
7	EtOH	13	20	94
8	EtOH	-	12 h	No reaction

<sup>a</sup> Isolated yield; Conditions of reaction: *o*-phenylenediamine (1 mmol), and benzyl (mmol), room temperature

**Table 2.** synthesis of quinoxaline in the presence of Fe<sub>3</sub>O<sub>4</sub>@APTES@MOF-199

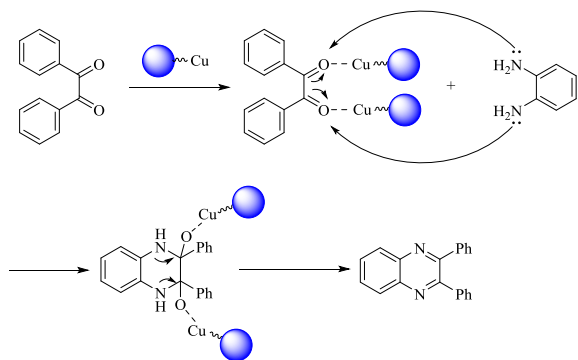
Entry	Diamine	Product	Time (min)	TON	Yield (%)	M.p. °C (Lit)
1			20	204.3	94	129-131 [46]
2			35	195.6	90	190-192 [46]
3			10	210.9	97	116-118 [46]
4			10	202.2	93	175-177 [47]
5			20	197.8	91	186-188 [47]
6			40	191.3	88	166-168 [48]
7			40	193.5	89	162-164 [48]
8			10	189.1	87	150-151 [46]

9			20	206.5	95	145-147 [46]
10			15	204.3	94	132-134 [46]
11			30	200.0	92	190-191 [47]
12			25	195.6	90	151-152 [47]
13			20	202.2	93	138-140 [47]
14			20	204.3	94	195-197 [47]
15			15	193.5	89	136-138 [49]
16			10	195.6	90	164-165 [49]

17			30	191.3	88	176-178 [49]
18			20	182.6	84	114-115 [46]
19			20	184.8	85	213-214 [46]
20			10	206.5	95	209-210 [46]

The recovered  $\text{Fe}_3\text{O}_4@\text{APTES}@\text{MOF-199}$  catalyst was also characterized by scanning electron microscopy. The SEM of reused catalyst after a fifth run shows nano size crystals during the course of the reaction (**Fig. 7**). These results indicated that the  $\text{Fe}_3\text{O}_4@\text{APTES}@\text{MOF-199}$  exhibited excellent reusability in the synthesis of quinoxaline.

However, ICP analysis was conducted on the magnetic nanocatalyst to identify the Cu content of the  $\text{Fe}_3\text{O}_4@\text{APTES}@\text{MOF-199}$  which was found to be 1.354 wt. %.



**Scheme 2.** The plausible reaction mechanism of  $\text{Fe}_3\text{O}_4@\text{APTES}@\text{MOF-199}$  for the synthesis of quinoxaline derivatives

#### 4. Conclusions

In conclusion, an effective  $\text{Fe}_3\text{O}_4@\text{APTES}@\text{MOF-199}$  catalyzed was investigated for the synthesis of quinoxaline derivatives. This catalyst was characterized by various techniques. In this study, we proposed this novel acidic nanocatalyst has great potential to be used as a promising catalyst with extensive applications in

different kinds of acid based catalytic reactions as a green, eco-friendly, non-toxic, economic and easy workup nanocatalyst with magnetic property which can be easily recovered by a simple magnet, and can be reused several times with no remarkable drop in the catalytic activity.

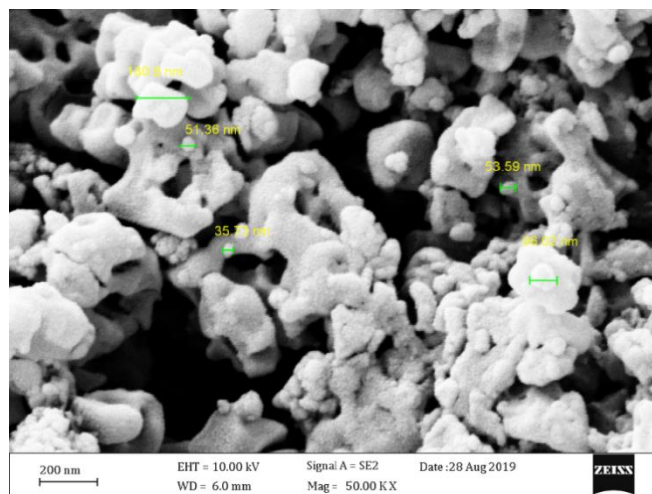


**Fig. 7.** Scanning electron microscopy of the reused  $\text{Fe}_3\text{O}_4@\text{APTES}@\text{MOF-199}$

#### Acknowledgements

The authors gratefully acknowledge partial support of this work by Payame Noor University (PNU) of Iran.

#### References

- [1] (a) R. G. Chaudhuri, S. Paria, *Chem. Rev.* 112, (2012) 2373-2433; (b) S. Sajjadifar, Z. Arzhegar, S. Khoshpoori, *J. Inorg. Organomet. Polym.* 28, (2018) 837-846; (c) Q.Y. Tamboli, S. M. Pathange, *Chem. Methodol.* 2, (2018) 73-82; (d) M. Soleiman-Beigi, Z. Arzhegar, *Monatsh. Chem.* 147,



- (2016) 1759-1763; (e) S. Sajjadifar, S. Rezayati, Z. Arzehgar, S. Abbaspour, M. Torabi Jafroudi, *J. Chin. Chem. Soc.* 65, (2018) 960-969.
- [2] W. Wu, Q. He, C. Jiang, *Nanoscale Res. Lett.* 3, (2008) 397-41.
- [3] D. Astruc, F. Lu, J. R. Aranzaes, *Angew. Chem. Int. Ed.* 44, (2005) 7852-7872.
- [4] C. Sun, J. S. Lee, M. Zhang, *Adv. Drug Deliv. Rev.* 60, (2008) 1252-1265.
- [5] X. Zheng, S. Luo, L. Zhang, J. P. Cheng, *Green Chem.* 11, (2009) 455-458.
- [6] Y. Jiang, C. Guo, H. Xia, I. Mahmood, C. Liu, H. Liu, *J. Mol. Catal. B: Enzym.* 58, (2009) 103-109.
- [7] A. H. Chughtai, N. Ahmad, H. A. Younus, A. Laypkov, F. Verpoort, *Chem. Soc. Rev.* 44, (2015) 6804-6849.
- [8] (a) J. Gascon, A. Corma, F. Kapteijn, F. X. Llabres, *ACS Catal.*, 4, (2014) 361-378; (b) Z. Arzehgar, V. Azizkhani, S. Sajjadifar, M. H. Fekri, *Chem. Methodol.* 3, (2019) 251-260; (c) Z. Arzehgar, S. Sajjadifar, H. Arandiyan, *Asian J. Green Chem.* 3, (2019) 43-52.
- [9] A. Dhakshinamoorthy, M. Alvaro, A. Corma, H. Garcia, *Dalton Trans.* 40, (2011) 6344-6360.
- [10] P. Deria, J. E. Mondloch, O. Karagiari, W. Bury, J. T. Hupp, O. K. Farha, *Chem. Soc. Rev.* 43, (2014) 5896-5912.
- [11] A. Dhakshinamoorthy, A. M. Asiric, H. Garcia, *Chem. Soc. Rev.* 44, (2015) 1922-1947.
- [12] (a) B. Panella, K. Hönes, U. Müller, N. Trukhan, M. Schubert, H. Pütter, M. Hirscher, *Angew. Chem. Int. Ed.* 47, (2008) 2138-2142; (b) S. Sajjadifar, Z. Arzehgar, A. Ghayuri, *J. Chin. Chem. Soc.*, 65, (2018) 205-211.
- [13] S. Navalon, A. Dhakshinamoorthy, M. Álvaro, H. Garcia, *ChemSusChem*, 6, (2013) 562-577.
- [14] L. T. Nguyen, C. V. Nguyen, G. H. Dang, K. K. Le, N. T. Phan, *J. Mol. Catal. A Chem.* 349, (2011) 28-35.
- [15] A. Dhakshinamoorthy, M. Alvaro, H. García, *ACS Catal.* 1, (2010) 48-53.
- [16] Z. Arzehgar, H. Ahmadi, *J. Chin. Chem. Soc.* 66, (2019) 303-306.
- [17] F. X. L. i Xamena, A. Abad, A. Corma, H. Garcia, *J. Catal.* 250, (2007) 294-298.
- [18] S. Gao, N. Zhao, M. Shu, S. Che, *Appl. Catal. A Gen.* 388, (2010) 196-201.
- [19] Y. Zhou, J. Song, S. Liang, S. Hu, H. Liu, T. Jiang, B. Han, *J. Mol. Catal. A Chem.* 308, (2009) 68-72.
- [20] S. Neogi, M. K. Sharma, P. K. Bharadwaj, *J. Mol. Catal. A Chem.* 299, (2009) 1-4.
- [21] K. K. Tanabe, S. M. Cohen, *Inorg. Chem.* 49, (2010) 6766-6774.
- [22] J. L. Rowsell, O. M. Yaghi, *Micropor. Mesopor. Mat.* 73, (2004) 3-14.
- [23] G. Zhao, N. Qin, A. Pan, X. Wu, C. Peng, F. Ke, M. Iqbal, K. Ramachandriah, J. Zhu, *J. Nanomater.* 2019, (2019) 1-11.
- [24] X. Zhao, S. Liu, Z. Tang, H. Niu, Y. Cai, W. Meng, F. Wu, J. P. Giesy, *Sci. Rep.* 5, (2015) 11849-11858.
- [25] M. E. Mahmoud, M. F. Amira, S. M. Seleim, A. K. Mohamed, *J. Hazard. Mater.* 381, (2020) 120979-120989.
- [26] R. Ricco, L. Malfatti, M. Takahashi, A. J. Hill, P. Falcaro, *J. Mater. Chem. A* 1, (2013) 13033-13045.
- [27] P. Ghosh, A. Mandal, *Adv. Appl. Sci. Res.* 2, (2011) 255-260.
- [28] M. González, H. Cerecetto, *Expert Opin. Ther. Pat.* 22, (2012) 1289-1302.
- [29] S. Sadegh-Malvajerd, Z. Arzehgar, F. Nikpour, *Z. Naturforsch. B* 68, (2013) 182-186.
- [30] S. B. Patel, B. D. Patel, C. Pannecouque, H. G. Bhatt, *Eur. J. Med. Chem.* 117, (2016) 230-240.
- [31] S. Dailey, J. W. Feast, R. J. Peace, I. C. Sage, S. Till, E. L. Wood, *J. Mater. Chem.* 11, (2001) 2238-2243.
- [32] D. M. Ruiz, J. C. Autino, N. Quaranta, P. G. Vazquez, G. P. Romanelli, *Sci. World J.* 2012, (2011) 1-8.
- [33] W. X. Guo, H. L. Jin, K. X. Chen, F. Chen, J. C. Ding, H. Y. Wu, *J. Braz. Chem. Soc.*, 20, (2009) 1674-1679.
- [34] M. M. Heravi, S. Taheri, K. Bakhtiari, H. A. Oskooie, *Catal. Commun.* 8, (2007) 211-214.
- [35] (a) A. Samimi, S. Zarinabadi, A. H. S. Kootenaei, A. Azimi, M. Mirzaei, *J. Med. Chem. Sci.* 3, (2020) 79-94; (b) Z. Moghadasi, *J. Med. Chem. Sci.* 2, (2019) 35-37.
- [36] S. Ajaikumar, A. Pandurangan, *Appl. Catal. A: Gen.* 357, (2009) 184-192.
- [37] S. Rezayati, M. Mehmannaavaz, E. Salehi, S. Haghi, R. Hajinasiri, S. Afshari Sharif Abad, *J. Sci. I. R. Iran* 27, (2016) 51-63.
- [38] S. Sajjadifar, I. Amini, T. Amoozadeh, *Chem. Methodol.* 1, (2017) 1-10.
- [39] S. Sajjadifar, M. A. Zolfigol, G. Chehardoli, S. Miri, P. Moosavi, *Int. J. Chemtech Res.* 5, (2013) 422-429.
- [40] J. S. Yadav, B. V. S. Reddy, K. Premalatha, K. S. Shankar, *Synthesis*, 23, (2008) 3787-3792.
- [41] H. R. Darabi, F. Tahoori, K. Aghapoor, F. Taala, F. J. Mohsenzadeh, *Braz. Chem. Soc.*, 19, (2008) 1646-1652.
- [42] M. M. Heravi, M. H. Tehrani, K. Bakhtiari, H. A. Oskooie, *Catal. Commun.* 8, (2007) 1341-1344.
- [43] S. Sajjadifar, Z. Gheisarzadeh, *Appl. Organomet. Chem.* 2019, 33, e4602.
- [44] (a) H. Sun, H. Zhang, H. Mao, B. Yu, J. Han, G. Bhat, *Environ. Chem. Lett.* 17, (2019) 1091-1096; (b) S. Chatterjee, N. Guha, S. Krishnan, A. K. Singh, P. Mathur, D. K. Rai, *Sci. Reports*, 10, (2020) 1-11; (c) D. J. Tranchemontagne, J. R. Hunt, O. M. Yaghi, *Tetrahedron* 64, (2008) 8553-8557.
- [45] A. Ghorbani-Choghamarani, B. Tahmasbi, N. Noori, R. Ghafouri nejad, *J. Iran. Chem. Soc.* 14, (2017) 681-693.
- [46] S. Bhargava, P. Soni, D. Rathore, *J. Mol. Struct.* 1198, (2019) 126758.
- [47] A. Hasaninejad, A. Zare, M. R. Mohammadzadeh and Z. Karami. *J. Iran. Chem. Soc.*, 6, (2009) 153-158.
- [48] A. Hasaninejad, A. Zare, M. R. Mohammadzadeh, M. Shekouhy, *Arkivoc* 13, (2008) 28-35.
- [49] M. M. Heravi, K. Bakhtiari, M. H. Tehrani, N. M. Javadi, H. A. Oskooie. *Arkivoc* 16, (2006) 16-22.